EMBO reports

EMBO open

scientific report

Structure and functional relevance of the Slit2 homodimerization domain

Elena Seiradake[1,2†], Anne C. von Philipsborn[3], Maud Henry[1,2], Martin Fritz[3], Hugues Lortat-Jacob[4], Marc Jamin[2], Wieger Hemrika[5], Martin Bastmeyer[3], Stephen Cusack[1,2] & Andrew A. McCarthy[1,2+]

[1]European Molecular Biology Laboratory, Grenoble Outstation, Grenoble, France, [2]Unit of Virus Host-Cell Interactions, UJF-EMBL-CNRS, UMR 5233, Grenoble, France, [3]Zoologisches Institut, Universitaet Karlsruhe (TH), Zell- und Neurobiologie, Karlsruhe, Germany, [4]IBS, Institut de Biologie Structurale, UMR 5075 CNRS-CEA-UJF, Grenoble, France, and [5]U-Protein Express B.V. Padualaan 8, Utrecht, The Netherlands

This is an open-access article distributed under the terms of the Creative Commons Attribution License, which permits distribution, and reproduction in any medium, provided the original author and source are credited. This license does not permit commercial exploitation without specific permission.

Slit proteins are secreted ligands that interact with the Roundabout (Robo) receptors to provide important guidance cues in neuronal and vascular development. Slit–Robo signalling is mediated by an interaction between the second Slit domain and the first Robo domain, as well as being dependent on heparan sulphate. In an effort to understand the role of the other Slit domains in signalling, we determined the crystal structure of the fourth Slit2 domain (D4) and examined the effects of various Slit2 constructs on chick retinal ganglion cell axons. Slit2 D4 forms a homodimer using the conserved residues on its concave face, and can also bind to heparan sulphate. We observed that Slit2 D4 frequently results in growth cones with collapsed lamellipodia and that this effect can be inhibited by exogenously added heparan sulphate. Our results show that Slit2 D4–heparan sulphate binding contributes to a Slit–Robo signalling mechanism more intricate than previously thought.

Keywords: neurons; guidance cues; signalling

EMBO reports (2009) **10**, 736–741. doi:10.1038/embor.2009.95

[1]European Molecular Biology Laboratory, Grenoble Outstation, and
[2]Unit of Virus Host-Cell Interactions, UJF-EMBL-CNRS, UMR 5233, 6 rue Jules Horowitz, 38042 Grenoble Cedex 9, France
[3]Zoologisches Institut, Universitaet Karlsruhe (TH), Zell- und Neurobiologie, Haid-und-Neu-Strasse 9, 76131 Karlsruhe, Germany
[4]IBS, Institut de Biologie Structurale, UMR 5075 CNRS-CEA-UJF, 41 rue Horowitz, 38027 Grenoble Cedex 01, France
[5]U-Protein Express B.V. Padualaan 8, 3584 CH Utrecht, The Netherlands
[†]Present address: The Division of Structural Biology, Henry Wellcome Building for Genomic Medicine, Roosevelt Drive, Oxford OX3 7BN, UK
[+]Corresponding author. Tel: +33 476 207276; Fax: +33 476 207199; E-mail: andrewmc@embl.fr

Received 21 October 2008; revised 31 March 2009; accepted 2 April 2009; published online 5 June 2009

INTRODUCTION

Slit ligand proteins secreted by the midline are important in neuronal development as they mediate a change in axonal response from attraction to repulsion. This change occurs when Slit binds to the transmembrane Roundabout (Robo) receptors of commissural neurons that have crossed the spinal cord floorplate (reviewed in Dickson & Gilestro, 2006). The Slits are large multi-domain proteins characterized by four consecutive leucine-rich repeat (LRR) domains (D1–D4) at their amino terminus. The minimal component required for Slit–Robo signalling is the N-terminal LRR region of Slit2 (Chen *et al*, 2001; Nguyen Ba-Charvet *et al*, 2001), specifically Slit D2 (Howitt *et al*, 2004) and a fragment spanning Robo domains Ig1 and Ig2 (Ig1–2; Liu *et al*, 2004). The structure of Slit2 D2 bound to Robo1 Ig1 showed that these domains interact through highly conserved electrostatic and hydrophobic regions (Morlot *et al*, 2007b). Heparan sulphate (HS), a highly charged polysaccharide, is essential in the repulsive guidance activities of Slit2 (Hu, 2001; Inatani *et al*, 2003), and Syndecan, a transmembrane protein containing HS, was later identified as a necessary component for Slit–Robo signalling (Johnson *et al*, 2004; Steigemann *et al*, 2004). Heparin, a chemically related analogue of HS, binds to both Slit2 D2 and Robo Ig1–2 (Hussain *et al*, 2006). In fact, the recent structure of *Drosophila* Robo Ig1–2 in complex with heparin shows that the Robo and Slit D2 heparin-binding sites are in close proximity, resulting in a continuous binding patch (Fukuhara *et al*, 2008). These results suggest that HS forms an integral part of the Slit–Robo signalling complex.

Slit dimerization is mediated by D4 and might be important for Slit–Robo signalling (Howitt *et al*, 2004). Here, we present the structure of the Slit2 D4 domain and show that it forms a stable non-symmetrical dimer through highly conserved residues on its concave face. Functional studies on the effect of Slit2 constructs on chick retinal–ganglion-cell (RGC) axons show that a Slit2

©2009 EUROPEAN MOLECULAR BIOLOGY ORGANIZATION

fragment spanning domains D2–D4, as well as the individual domains D2 and D4, elicits a response *in vitro*. Furthermore, we show that Slit2 D4 can bind to HS *in vitro* and that exogenously added HS can inhibit the collapse response of chick RGC growth cones to Slit2 D4. Taken together, these results provide compelling evidence that Slit2 dimerization is functionally relevant and that heparin binding to Slit2 is more complex than understood earlier.

RESULTS AND DISCUSSION

Overall structure

The Slit2 D4 structure was solved by molecular replacement using a modified model of human Slit2 D3 (Morlot *et al*, 2007a) and was refined at 1.8 Å resolution. The crystallographic asymmetrical unit contains two molecules in an anti-parallel dimeric arrangement. Each monomer adopts a slightly curved right-handed LRR fold similar to that of other Slit2 LRR domains (Morlot *et al*, 2007a, b). Slit2 D4 has five LLRs and two flanking cysteine-rich capping domains (Fig 1A). The concave face is composed of a continuous seven-stranded β-sheet. The first two β-strands are anti-parallel and form the N-terminal cap, whereas each of the five LRRs contributes a parallel β-strand. The convex surface is composed of variable loops and short helices. As seen for Slit2 D2 and D3, the N-terminal cap is a double hairpin stabilized by two disulphide bridges, whereas the carboxy-terminal cap adopts an irregular fold containing a 12-residue α-helix, two 3_{10} helices and two disulphide bridges.

Slit2 D4 dimer

Multi-angle laser light scattering (MALLS) confirmed that Slit2 D4 exists as a homodimer in solution (data not shown). The dimer has a compact globular shape (30 Å × 60 Å × 70 Å) (Fig 1B) and shows a quaternary structure resembling that of the extracellular-matrix protein decorin (Fig 1C,D; Scott *et al*, 2004). Both decorin and Slit2 D4 dimerize through their concave face, but in distinct ways. The decorin dimer is mainly formed by interactions involving the N-terminal capping domain, LRR1 and the central LRRs, but not the C-terminal LRRs. In Slit2 D4, the entire domain, including the C-terminal cap, is involved. In addition, unlike decorin, the Slit2 D4 dimer is not perfectly symmetrical, as the two monomers differ in conformation ($\text{r.m.s.d.}_{181C\alpha} = 0.45$ Å). The most significant difference occurs between residues 875 and 881, where the Cα positions deviate by as much as 2.4 Å. This region corresponds to the 'β-switch' loop, which adopts different conformations in the free and ligand-bound structures of glycoprotein Ib-α (Huizinga *et al*, 2002) and which characterizes this class of LRR domains.

The dimer interface

Dimerization buries 1,240 Å^2 of the solvent-accessible surface for each monomer of Slit2 D4. This represents 13.6% of the total surface, which is significantly larger than the buried Slit2 D2 surface on binding to Robo1 Ig1 (657 Å^2). Dimerization involves mainly electrostatic interactions, but several hydrophobic residues from LRR 2–5 and the C-terminal capping domain (Leu 781, Ile 807, Leu 829, Ala 855, Ile 883, Leu 896 and Leu 898) also participate. An important feature of the dimer interface is the β-switch loop, which reaches deep into the concave surface of the opposite monomer, forming extensive intermolecular contacts (Fig 2A–C). The atomic *B*-factors of the loop are comparatively higher in one of the two monomers, suggesting that the dimer tolerates flexibility within its interface, a property linked to high affinity (Seiradake *et al*, 2006).

The dimer interface contains a total of 11 direct intermolecular hydrogen bonds. Arg 885 contributes six of these by forming a salt bridge with Asp 762 and Asp 783 and a hydrogen bond with Ser 785 (Fig 2D). Arg 828 and Glu 877 form an additional salt bridge, which is non-symmetrical because of differences in the two β-switch loops (Fig 2A,B). Similarly, there are non-symmetrical hydrogen bonds involving His 853: to avoid steric clashes with the adjacent β-switch loop, the two His 853 side chains hydrogen bond to either the Ser 852 or the Tyr 878 carbonyl group (Fig 2C). This results in the His 853 imidazole ring of monomer A becoming sandwiched between Pro 881 and the His 853 imidazole ring of monomer B. Two additional hydrogen bonds are observed between Tyr 760 and Thr 899, with the Tyr side chain also maintaining hydrophobic interactions. Last, 18 well-ordered water molecules mediate an extensive network of hydrogen bonds, which further stabilize the dimer interface (Fig 2E).

Heparan sulphate binding

The surface of the Slit2 D4 homodimer shows a striking electrostatic potential distribution, with the top surface being highly negatively charged and the bottom mainly positively charged (Fig 3A,C). More specifically, the bottom face shows three basic patches, one from each monomer and one from the dimer interface. Contributing to these patches are residues Lys 746, Arg 788, Arg 812 and Arg 814. The distribution of basic residues extends around the sides to cover the N-terminal half of each molecule in the dimer (Fig 3C). Here, the contributing residues include Lys 750, Arg 754, Lys 771 and Lys 777. In the basic patch at the dimer interface, we observe a well-ordered sulphate ion (Fig 3A,C). This ion is held tightly in place, forming hydrogen bonds with Tyr 810 and His 833 from each monomer and four water-mediated hydrogen bonds with the protein backbone (Fig 2F).

Heparin is an integral part of Slit–Robo signalling and has been shown to bind to Slit2 D2, the C-terminal cysteine-knot domain of Slit2 and Robo1 Ig1–2. Although heparin has not been implicated in binding to Slit2 D4, the large basic regions and the conspicuous sulphate-binding site suggest a possible interaction. To test this hypothesis, we carried out surface plasmon resonance experiments in which either Slit2 D2 or Slit2 D4 was flowed over a HS-conjugated sensor chip. We observed a strong interaction between Slit2 D4 and HS, characterized by a dissociation constant (K_d) of 50 nM (supplementary Fig S5B online). Although this domain binds to HS more weakly than Slit2 D2 ($K_d = 10$ nM; supplementary Fig S5C online), the results nevertheless support our structure-based hypothesis and we were able to reduce HS binding by reversing the charge of the large basic region on the bottom face (data not shown).

Biological activity of Slit2 constructs

Full-length Slit2 and Slit2 D2 have previously been shown to cause the collapse of chick and *Xenopus* RGC axon growth cones (Hussain *et al*, 2006; Piper *et al*, 2006). We carried out similar *in vitro* assays with our Slit2 constructs on chick RGCs and tested them in a 'stripe and collapse' assay. When presented in substrate-bound form, the Slit2 D2–D4 fragment (encompassing D2, D3 and

©2009 EUROPEAN MOLECULAR BIOLOGY ORGANIZATION

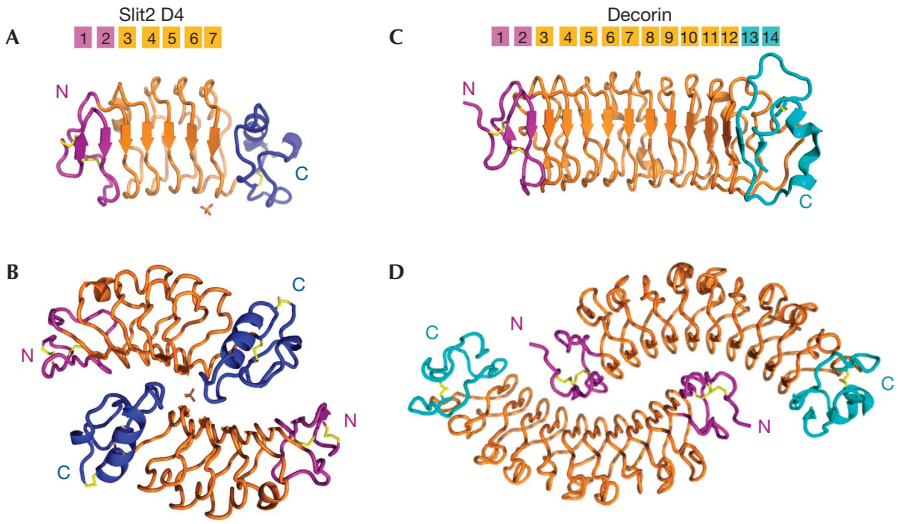

Fig 1 | Structure of Slit2 D4 and the Decorin dimer in similar orientations. The Slit2 D4 and decorin amino-terminal caps are coloured purple, whereas their carboxy-terminal caps are coloured blue and cyan. The LRRs are coloured orange and the disulphide bridges are in yellow (Slit2 D4 N-terminal cap: Cys 727–Cys 733 and Cys 731–Cys 740; Slit2 D4 C-terminal cap: Cys 863–Cys 886 and Cys 865–Cys 907). The sulphate ion is indicated by sticks. (**A**) Human Slit2 D4 monomer. (**B**) Human Slit2 D4 dimer. (**C**) Bovine decorin monomer. (**D**) Bovine decorin dimer.

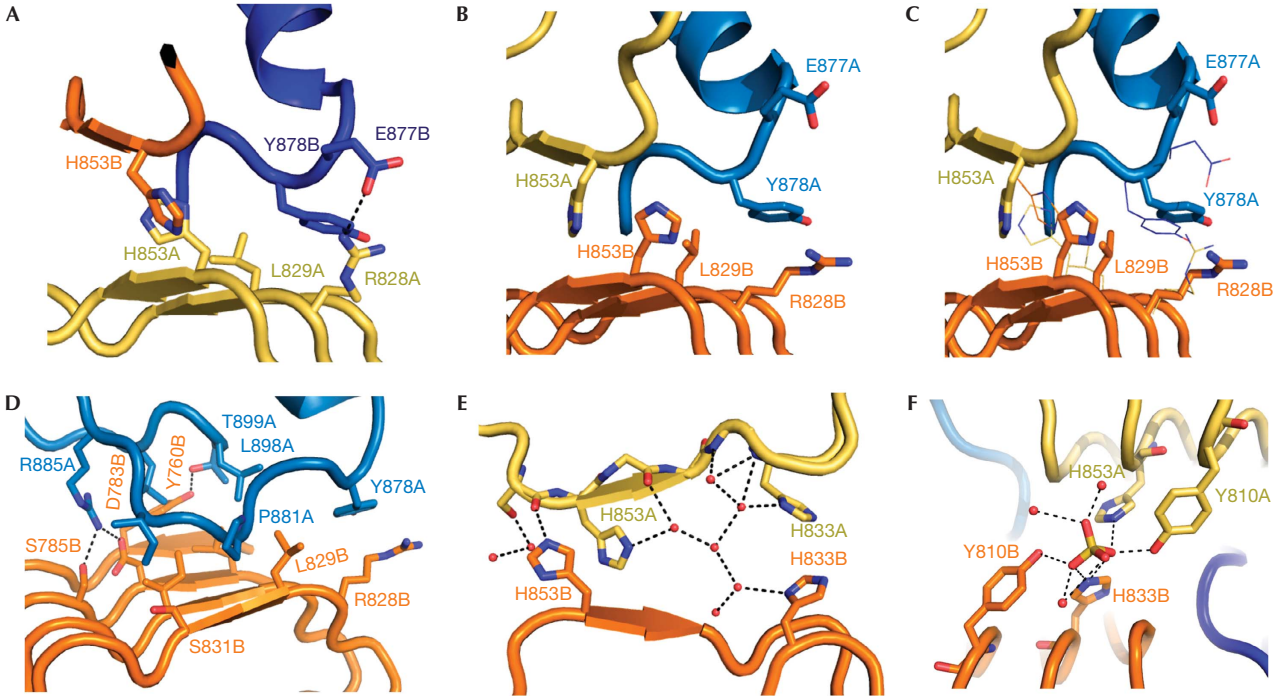

Fig 2 | Molecular interactions at the dimer interface. (**A**) Central region of the Slit2 D4 dimerization interface. Residues that differ in chains (**A**) and (**B**) are shown as sticks. The β-switch loop of chain (**B**) is coloured purple. (**B**) The asymmetric dimer region with the chain (**A**) β-switch loop is coloured purple. (**C**) Chain (**A**) and (**B**) superpositions. The orientation of the ribbon and sticks model is as in (**B**) (chain (**A**) on top, chain (**B**) at the bottom). Lines represent the alternative residue conformation in the opposite chains, as seen in (**A**). (**D**) The β-switch loop of chain (**A**) and interacting residues. (**E**) The central four-histidine cluster and water network. (**F**) The sulphate binding site.

D4), Slit2 D2 and Slit2 D4 are all equally avoided by growing axons that can choose between the respective Slit2 construct and laminin (data not shown) or FC (fragment constant, Fig 4A), a neutral protein substrate. In the collapse assay, both soluble Slit2 D2–4 (data not shown) and Slit2 D2 resulted in typical growth cone collapse with fully retracted lamellipodia and filopodia (Fig 4B). Here, Slit2 D2–4 induced a collapse of more than 75% of the growth cones at protein concentrations 5–10 times lower than

©2009 EUROPEAN MOLECULAR BIOLOGY ORGANIZATION

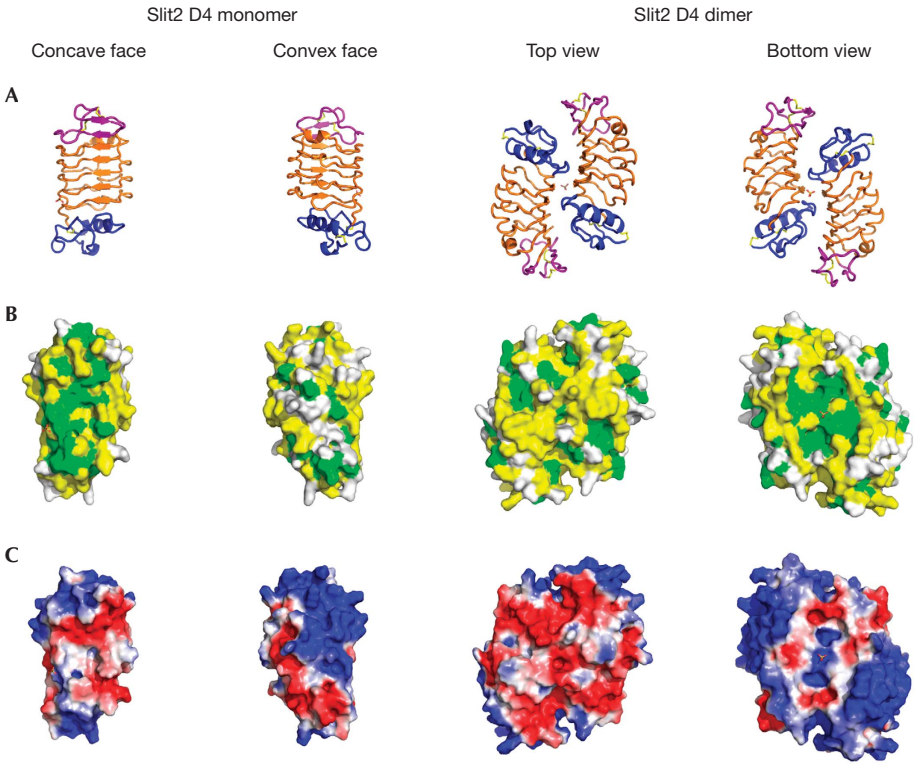

Fig 3 | Sequence conservation and electrostatic surface representation of Slit2 D4 with the sulphate ion in sticks. (**A**) Structural representation, in four orientations and coloured as in Fig 1. (**B**) Sequence surface conservation as viewed in (**A**) and coloured in green: identical; yellow: partly conserved; white: poorly conserved. (**C**) Electrostatic surface potential calculated with Adaptive Poisson–Boltzmann Solver (APBS; Baker *et al*, 2001; from −2 coloured in red: negatively charged, to +2 coloured in blue: positively charged).

those used with the Slit2 D2 domain (data not shown). Slit2 D4 also affected the growth of chick RGCs at concentrations similar to those used with Slit2 D2. In this case, however, the majority of the growth cones showed a 'bare branch morphology', characterized by elongated filopodia and collapsed lamellipodia (Fig 4B). Quantifications of growth-cone responses to the different Slit2 constructs are given in Fig 4C.

Soluble heparin inhibits the collapse of *Xenopus* RGCs induced by full-length Slit2 but not by Slit2 D2 (Hussain *et al*, 2006). This led to the conclusion that heparin might have a dual function in Slit–Robo signalling, reflecting the heparin-binding properties of the Slit2 D2 and Slit2 CT domains. In line with this, we find that soluble HS oligomers (12-mers) inhibit the collapse of chick RGC growth cones induced by Slit2 D2–4 (data not shown). We also found a partial reduction of Slit2 D2-induced collapse by HS oligomers ($P<0.005$; χ^2-test). More interesting is the fact that the addition of HS oligomers to the cell-culture medium abolished the bare branch morphology of growth cones induced by Slit2 D4 and led to a morphology indistinguishable from controls using HS oligomers alone ($P<0.005$; χ^2-test) (Fig 4C).

Slit D4 sequence comparison

Slit D4 domains are highly conserved among bilateral organisms (for example, human Slit2 D4 has 98% and 53% sequence identity to its murine and *Drosophila* orthologues; supplementary Fig S6 online). The most highly conserved residues map to the concave dimerization surface of the molecule, whereas the convex face is much less conserved (Fig 3B). The conservation of residues in the D4 dimer interface and the large, accessible surface area buried on dimerization (~2,500 Å^2) strongly suggest that all Slit family members dimerize in a similar manner through the fourth LRR domain. Out of the 21 residue positions involved in dimerization, 11 are invariant across the sequence alignment, including a continuous motif comprising residues 882–886 within the β-switch loop. Seven residue positions are either identical or show highly conservative substitutions across homologues. Only three positions show chemically significant variations: two (Leu 781 and Glu 877) are located at the periphery of the dimer interface, whereas the third (Lys 879) participates in dimer formation exclusively through main-chain atoms. Hence, variations at these positions are not expected to significantly compromise dimerization. In addition, our attempts to disrupt the dimerization interface by multiple mutageneses have so far failed, indicating a high stability of the dimer (supplementary information online).

The sulphate-binding residues, Tyr 810 and His 833 (which are integral to the dimerization interface), are strictly conserved across the Slit D4 domains. By contrast, the potential heparin-binding residues on the bottom face (Lys 746, Arg 788, Arg 812 and Arg 814) and those on the N-terminal convex face (Lys 750, Arg 754, Lys 771 and Lys 777) are less well conserved in other Slit family members (supplementary Fig S6 online). In fact only three of these seven residues are conserved in *Drosophila*. This might

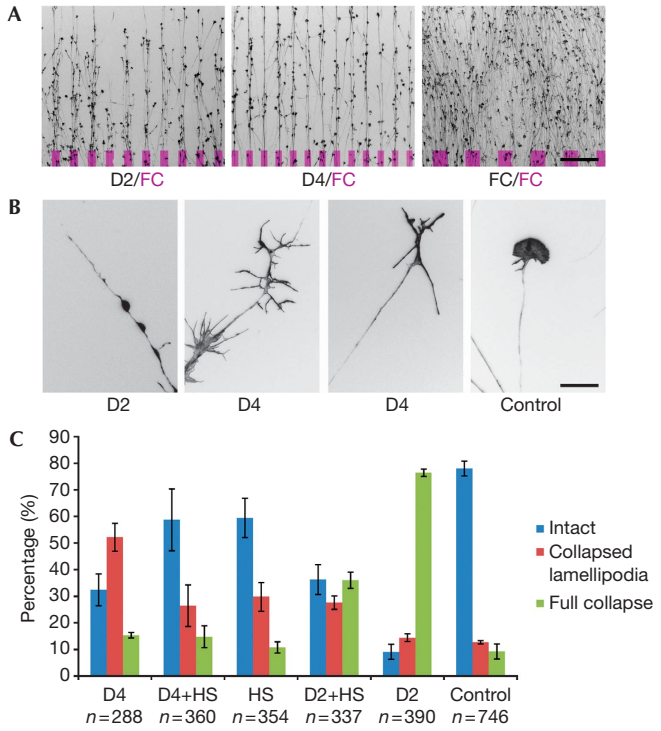

Fig 4 | Biological activity of Slit2 contructs. (**A**) Stripe assay with axons given the choice between substrate-bound lanes covered with Slit2 D2, Slit2 D4 and FC compared with lanes covered with FC (indicated in magenta). Scale bar, 200 μm. (**B**) Representative single growth cones after treatment with soluble Slit2 D2 (full collapse), Slit2 D4 (bare branch morphology) and control treatment (intact morphology). Scale bar, 20 μm. (**C**) Heparan sulphate (HS) oligomers (12-mers) alter the effect of Slit2 D2 and D4 on growth cones incubated for 15 min with 100 μg/ml HS oligomers, followed by incubation for 30 min with 100 μg/ml HS oligomers and 50 μg/ml Slit2 D2 or D4, respectively. Blue bars indicate the percentage of intact growth cones, red bars indicate growth cones with bare branch morphology and green bars indicate fully collapsed growth cones. Bars indicate the s.e.m.; *n* indicates the number of growth cones scored.

explain why no heparin interaction with *Drosophila* Slit D4 was observed (Hussain *et al*, 2006). The heparin-binding potential of the fourth LRR domain is therefore likely to vary among Slit homologues, which might be important for modulating the functional properties of different Slits.

A functional role for Slit2 D4

Our *in vitro* assays show that chick RGCs were responsive to similar concentrations of Slit2 D2 and D4. In contrast to Slit2 D2, which leads to a full collapse and retraction of the growth cone, Slit2 D4 has a less pronounced effect, collapsing only lamellipodia and leaving filopodia mainly intact. We also observed that Slit2 D2–D4 fragment elicited growth cone collapse at much lower concentrations than Slit2 D2. Thus, although dimerization might not be essential for an axonal response, it clearly has a potentiating effect. How Slit2 D4 elicits a response is unclear, as Slit2 D4 is not known to bind to a Robo receptor and does not bind to Robo1 (data not shown). One possibility is that the interaction of Slit2 D4 with cell-surface HS elicits a response. Such an interaction might feasibly be mediated by Syndecan, which is known to be important for Slit–Robo signalling in *Drosophila* (Johnson *et al*, 2004; Steigemann *et al*, 2004). These studies suggested that Syndecan acts as a co-receptor by presenting Slit to Robo and stabilizing the complex, but the possibility that the highly conserved cytoplasmic domains of Syndecan might have a more subtle modulatory function was not ruled out.

More recent studies support the Slit–Robo HS stabilizing effect, where the loss in response of *Xenopus* RGC axons towards Slit2 D2 on treatment with heparinase 1 can be reversed by the addition of soluble heparin (Hussain *et al*, 2006). However, it is not understood why chick and *Xenopus* RGCs are unresponsive to full-length Slit2 constructs incubated with heparin but remain responsive to heparin-incubated Slit2 D2. This has been suggested to be because heparin has a dual role in signaling: modulating the Slit2 distribution through its CT region; and participating in a ternary Slit2–Robo1–heparin complex that is necessary for signalling (Hussain *et al*, 2006). In our studies, Slit2 D2–4 complex, which lacks the CT region, Slit2 D4 and, at least partly, Slit2 D2 remain sensitive to incubation with HS. These results are indicative of a more complex signalling mechanism that involves HS.

Syndecans are better known as co-receptors but they have been shown to signal independently (Couchman, 2003). In *Caenorhabditis elegans* it has been reported that SAX-3/Robo has a SLT-1/cSlit1 independent function, which is dependent on certain heparin modifications (Bulow & Hobert, 2004), and that Syndecan can function autonomously in axon guidance (Rhiner *et al*, 2005). Syndecan can also regulate neuronal growth-cone signalling by interacting with other HS receptors, such as the leukocyte-common antigen-related (LAR)-receptor tyrosine phosphatase in *Drosophila* (Fox & Zinn, 2005). In addition, others have shown that Robo can bind to heparin alone (Hussain *et al*, 2006; Fukuhara *et al*, 2008). Our observation that Slit2 D4 is active on growing RGC axons in a HS-dependent manner raises the possibility that Slit2 D4 might interact with Syndecan to induce a partial cytoskeletal rearrangement, resulting in the bare branch morphology. Indeed, other HS-binding receptors at the cell surface, such as LAR or Robo, could also be implicated in modulating such a signal. In conclusion, our results show an important role for Slit2 dimerization through Slit2 D4. Furthermore, that purified Slit2 D4 has a HS-dependent effect suggests that D4 has a more complex part in Slit2 signalling than as a simple dimerization module. Clearly, further studies are required to identify the HS-dependent interaction partners of Slit2 D4 on the cell surface.

METHODS

Preparation of Slit2 domains. Human Slit2 constructs (Slit2 D2 (residues 271–479), Slit2 D4 (residues 726–907) and Slit2 D2–4 (residues 271–907)) were essentially produced and purified as described earlier (Morlot *et al*, 2007a). Further detail can be found in the supplementary information online.

Crystallization and X-ray data collection of Slit2 D4. Purified and deglycosylated Slit2 D4 was crystallized from solutions containing 0.2 M $LiSO_4$, 0.1 M Tris pH 8.5 and 30% polyethyleneglycol 4000. The crystals were frozen in a cryoprotectant solution

©2009 EUROPEAN MOLECULAR BIOLOGY ORGANIZATION

containing all solution components and 10–15% glycerol, and diffraction data were collected at the European Synchrotron Radiation Facility (Grenoble, France; beamline ID14-EH4). Further details can be found in the supplementary information online.

Growth cone stripe and collapse assays. RGCs were dissected and cultivated overnight in F12 medium on a laminin-coated coverslip. To test the effect of a protein, the protein solution was mixed with culture medium. The culture medium of the explants was exchanged with the protein-containing medium and the cultures were incubated for 30 min at 37 °C. To test the inhibitory effect of HS the RGCs were first incubated with fresh medium containing HS, followed by incubation with medium containing HS and protein solution. The cultures were then fixed, stained with fluorescently labelled phalloidin and photographed for growth-cone collapse evaluation. For the stripe assay, the protein was not added to the culture medium after outgrowth, but rather bound in a striped pattern onto the cover slip on which the axons were cultivated. To produce a striped pattern, a silicone matrix with small channels was placed on a coverslip and filled with protein solution. The pattern was then coated with laminin. To make the patterns visible, the protein of interest was mixed with a fluorescently labelled inactive protein. Further details on the *in vitro* stripe and collapse assays that were used to analyse the effect of Slit2 constructs on chick RGCs are described in the supplementary information online.

Surface plasmon resonance spectroscopy binding assay. HS was biotinylated at the reducing end and immobilized on a BiAcore (Uppsala, Sweden) sensorchip. One flow cell was left untreated and used as a negative control. For binding assays, the proteins were simultaneously injected over the control and the HS. Further details can be found in the supplementary information online.

Supplementary information is available at *EMBO reports* online (http://www.emboreports.org).

ACKNOWLEDGEMENTS
We thank C. Morlot for her assistance in the initial stage of this study, A. Schuller for help with the functional assays, R. Aricescu for providing technical advice and C. Petosa for critical reading of the paper. Partial funding for this project was provided by the European Union FP6 Integrated Project 'SPINE2-Complexes' and the Deutsche Forschungsgemeinschaft (BA 1034/14-2 to M.B.). E.S. was supported by a European Union FP6 Marie Curie Early Stage Research Training Fellowship under Contract MEST-CT-2004-504640 (E-STAR). The atomic coordinates and structure factors have been deposited in the Protein Data Bank (www.pdb.org) with the accession code: 2wfh.

CONFLICT OF INTEREST
The authors declare that they have no conflict of interest.

REFERENCES
Baker NA, Sept D, Joseph S, Holst MJ, McCammon JA (2001) Electrostatics of nanosystems: application to microtubules and the ribosome. *Proc Natl Acad Sci USA* **98:** 10037–10041
Bulow HE, Hobert O (2004) Differential sulfations and epimerization define heparan sulfate specificity in nervous system development. *Neuron* **41:** 723–736
Chen JH, Wen L, Dupuis S, Wu JY, Rao Y (2001) The N-terminal leucine-rich regions in Slit are sufficient to repel olfactory bulb axons and subventricular zone neurons. *J Neurosci* **21:** 1548–1556
Couchman JR (2003) Syndecans: proteoglycan regulators of cell-surface microdomains? *Nat Rev Mol Cell Biol* **4:** 926–937
Dickson BJ, Gilestro GF (2006) Regulation of commissural axon pathfinding by slit and its Robo receptors. *Annu Rev Cell Dev Biol* **22:** 651–675
Fox AN, Zinn K (2005) The heparan sulfate proteoglycan syndecan is an *in vivo* ligand for the Drosophila LAR receptor tyrosine phosphatase. *Curr Biol* **15:** 1701–1711
Fukuhara N, Howitt JA, Hussain SA, Hohenester E (2008) Structural and functional analysis of Slit and heparin binding to immunoglobulin-like domains 1 and 2 of *Drosophila* Robo. *J Biol Chem* **283:** 16226–16234
Howitt JA, Clout NJ, Hohenester E (2004) Binding site for Robo receptors revealed by dissection of the leucine-rich repeat region of Slit. *EMBO J* **23:** 4406–4412
Hu H (2001) Cell-surface heparan sulfate is involved in the repulsive guidance activities of Slit2 protein. *Nat Neurosci* **4:** 695–701
Huizinga EG, Tsuji S, Romijn RA, Schiphorst ME, de Groot PG, Sixma JJ, Gros P (2002) Structures of glycoprotein Ibalpha and its complex with von Willebrand factor A1 domain. *Science* **297:** 1176–1179
Hussain SA *et al* (2006) A molecular mechanism for the heparan sulfate dependence of slit–robo signaling. *J Biol Chem* **281:** 39693–39698
Inatani M, Irie F, Plump AS, Tessier-Lavigne M, Yamaguchi Y (2003) Mammalian brain morphogenesis and midline axon guidance require heparan sulfate. *Science* **302:** 1044–1046
Johnson KG, Ghose A, Epstein E, Lincecum J, O'Connor MB, Van Vactor D (2004) Axonal heparan sulfate proteoglycans regulate the distribution and efficiency of the repellent slit during midline axon guidance. *Curr Biol* **14:** 499–504
Liu Z, Patel K, Schmidt H, Andrews W, Pini A, Sundaresan V (2004) Extracellular Ig domains 1 and 2 of Robo are important for ligand (Slit) binding. *Mol Cell Neurosci* **26:** 232–240
Morlot C, Hemrika W, Romijn RA, Gros P, Cusack S, McCarthy AA (2007a) Production of Slit2 LRR domains in mammalian cells for structural studies and the structure of human Slit2 domain 3. *Acta Crystallogr D Biol Crystallogr* **63:** 961–968
Morlot C, Thielens NM, Ravelli RB, Hemrika W, Romijn RA, Gros P, Cusack S, McCarthy AA (2007b) Structural insights into the Slit–Robo complex. *Proc Natl Acad Sci USA* **104:** 14923–14928
Nguyen Ba-Charvet KT, Brose K, Ma L, Wang KH, Marillat V, Sotelo C, Tessier-Lavigne M, Chedotal A (2001) Diversity and specificity of actions of Slit2 proteolytic fragments in axon guidance. *J Neurosci* **21:** 4281–4289
Piper M, Anderson R, Dwivedy A, Weinl C, van Horck F, Leung KM, Cogill E, Holt C (2006) Signaling mechanisms underlying Slit2-induced collapse of *Xenopus* retinal growth cones. *Neuron* **49:** 215–228
Rhiner C, Gysi S, Frohli E, Hengartner MO, Hajnal A (2005) Syndecan regulates cell migration and axon guidance in *C. elegans*. *Development* **132:** 4621–4633
Scott PG, McEwan PA, Dodd CM, Bergmann EM, Bishop PN, Bella J (2004) Crystal structure of the dimeric protein core of decorin, the archetypal small leucine-rich repeat proteoglycan. *Proc Natl Acad Sci USA* **101:** 15633–15638
Seiradake E, Lortat-Jacob H, Billet O, Kremer EJ, Cusack S (2006) Structural and mutational analysis of human Ad37 and canine adenovirus 2 fiber heads in complex with the D1 domain of coxsackie and adenovirus receptor. *J Biol Chem* **281:** 33704–33716
Steigemann P, Molitor A, Fellert S, Jackle H, Vorbruggen G (2004) Heparan sulfate proteoglycan syndecan promotes axonal and myotube guidance by slit/robo signaling. *Curr Biol* **14:** 225–230

SOME RIGHTS RESERVED
***EMBO reports* is published by Nature Publishing Group on behalf of European Molecular Biology Organization. This article is licensed under a Creative Commons Attribution-Noncommercial-Share Alike 3.0 License. [http://creativecommons.org/licenses/by-nc-sa/3.0/]**